

# Universal flow diagram for the magnetoconductance in disordered GaAs layers

S. S. Murzin<sup>1,2</sup>, M. Weiss<sup>1</sup>, A. G. M. Jansen<sup>1</sup> and K. Eberl<sup>3</sup>

<sup>1</sup>*Grenoble High Magnetic Field Laboratory, Max-Planck-Institut für Festkörperforschung and Centre National de la Recherche Scientifique, BP 166, F-38042, Grenoble Cedex 9, France*

<sup>2</sup>*Institute of Solid State Physics RAS, 142432, Chernogolovka, Moscow District., Russia*

<sup>3</sup>*Max-Planck-Institut für Festkörperforschung, Postfach 800 665 D-70569, Stuttgart, Germany*

The temperature driven flow lines of the diagonal and Hall magnetoconductance data ( $G_{xx}, G_{xy}$ ) are studied in heavily Si-doped, disordered GaAs layers with different thicknesses. The flow lines are quantitatively well described by a recent universal scaling theory developed for the case of duality symmetry. The separatrix  $G_{xy} = 1$  (in units  $e^2/h$ ) separates an insulating state from a spin-degenerate quantum Hall effect (QHE) state. The merging into the insulator or the QHE state at low temperatures happens along a semicircle separatrix  $G_{xx}^2 + (G_{xy} - 1)^2 = 1$  which is divided by an unstable fixed point at  $(G_{xx}, G_{xy}) = (1, 1)$ .

PACS numbers: 73.50.Jt; 73.61.Ey; 73.40.Hm

In spite of considerable efforts in theoretical and experimental research on the Quantum Hall Effect (QHE) for many years, the complete description of its evolution for decreasing temperature is still unsatisfactory at the moment. About 20 years ago a flow-diagram [1] for the coupled evolution of the diagonal ( $G_{xx}$ ) and Hall ( $G_{xy}$ ) conductivities was sketched for increasing sample size  $L$  (or, equivalently, increasing phase breaking length  $L_\phi$  for finite decreasing temperatures) on the basis of a two-parameter scaling approach to the QHE [2]. With increasing system size ( $L \rightarrow \infty$ )  $G_{xx}$  tends to zero ( $G_{xx} \rightarrow 0$ ) while  $G_{xy}$  becomes quantized ( $G_{xy} \rightarrow i$ ,  $i$  is an integer,  $G_{xx}$  and  $G_{xy}$  are in units  $e^2/h$ ). The points ( $G_{xx}(L), G_{xy}(L)$ ) flow on lines merging into the QHE plateau states characterized by one of the fixed points  $(0, i)$ . In addition there are unstable fixed points in between these plateaus at  $(G_{xx}^c, G_{xy}^c = i + 1/2)$  where the flow lines terminate, meaning that points with  $G_{xy} = i + 1/2$  maintain their Hall conductance for all  $L$ . Numerical calculations for a system of noninteracting electrons at high magnetic fields in the lowest Landau level give  $G_{xx}^c \approx 1/2$  in the presence of different random potentials [3]. For sufficiently low temperatures the  $(G_{xx}, G_{xy})$  data flow on a separatrix in the flow diagram which for a smooth disorder potential has been derived to be a semicircle of the form [4]

$$G_{xx}^2 + [G_{xy} - (i + 1/2)]^2 = 1/4, \quad (1)$$

with  $G_{xx}^c = 1/2$  and  $G_{xy}^c = i + 1/2$ .

Recently it has been shown [5] that the semicircle law follows solely from the consistency of the law of corresponding states, which was already used to deduce the complete set of fractional and integer quantum Hall states from the integer  $i = 1$  state [6]. Moreover, exact flow lines for the integer and fractional QHE were derived [7] from duality and particle-hole symmetries [8], which underlie the law of corresponding states. Their shape does not depend on details of the 2D system. The sep-

aratrix are the above given semicircles and the vertical lines  $G_{xy} = i + 1/2$ .

In the presented work we explore the temperature driven flow diagram of  $G_{xx}(T)$  versus  $G_{xy}(T)$  for disordered heavily Si-doped GaAs layers with different thicknesses from 40 to 27 nm in a large temperature range from 4.2 K down to 40 mK. At low temperatures these samples are situated in the transition region between a QHE state and an insulating state. For the temperature evolution a quantitative agreement is found with the universal theory [7] for the flow lines of the  $(G_{xx}, G_{xy})$  data points.

The temperature evolution of the flow diagram was already studied in many experiments [9], but showed inconsistencies with respect to theory. As an example, values reported for  $G_{xx}^c$  in the literature range from 0.02 up to 0.8 (for the transition  $i \rightarrow i + 1$ ), and even different values for different  $i$  on the same sample have been observed. The semicircle relation was observed in the dependence  $G_{xx}(G_{xy})$  with  $G_{xx}$  and  $G_{xy}$  driven by magnetic field in a SiGe-Ge-SiGe quantum well at rather high temperatures of 0.3-3 K. The position of the unstable fixed point however was essentially different from  $(1/2, 1/2)$  [10]. Although  $G_{xx}^c \approx 1/2$  and  $G_{xy}^c \approx i + 1/2$  were observed at the transition from the insulator to the quantum Hall state ( $i = 0$ ) in  $\delta$ -doped GaAs [11] and between two QHE plateaus with  $G_{xy} = 1$  and 2 ( $i = 1$ ) in a Si-Ge hole system [12], in most experiments these values differ significantly from  $1/2$  and  $i + 1/2$ , respectively.

There are several reasons leading to a difference between theoretical and experimentally observed critical values of  $G_{xx}^c$  and  $G_{xy}^c$ , like macroscopic inhomogeneities of the sample, enhanced current densities near the edges of even homogeneous samples (this explains probably the low values  $G_{xx}^c \approx 0.02$  observed in high mobility GaAs heterostructures) and spin effects.

The theory introduced in Ref. [7] has been developed for spinless (or totally spin polarized) electrons. Therefore, the most favorable candidate for an experimental

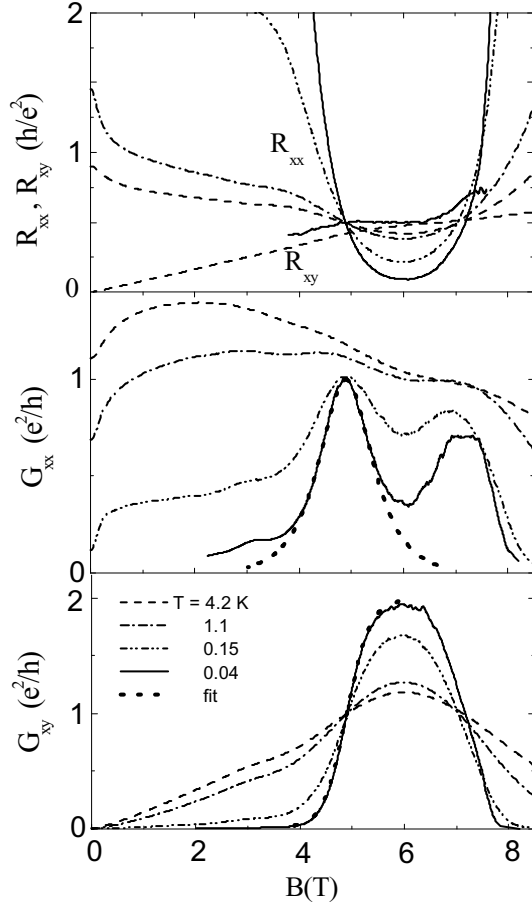


FIG. 1. Magnetic field dependence of the diagonal ( $R_{xx}$ , per square) and Hall ( $R_{xy}$ ) resistance and the diagonal ( $G_{xx}$ ) and Hall ( $G_{xy}$ ) conductance for sample 30 in a magnetic field perpendicular to the heavily doped GaAs layer at different temperatures. Dotted lines for  $G_{xx}$  and  $G_{xy}$  show the result of a theoretical fit around  $B_c = 4.9$  T.

study of the flow diagram under integer QHE conditions is a disordered system with a small  $g$ -factor such that the spin-splitting  $g\mu_B B$  ( $\mu_B$  is the Bohr magneton) is small with respect to the disorder broadening and will only show up in the flow diagram at rather low temperatures [13]. As we have shown in previous investigations on similar samples, electron-electron interaction cannot be neglected in the systems which are subject of the present work [14]. For  $G_{xx} > 1$  interaction mainly leads to temperature dependent flow of the  $(G_{xx}(T), G_{xy}(T))$  data [15] and a dependence of the localization length on interaction [14]. For  $k_B T \ll \mu_B g B$  ( $k_B$  is the Boltzmann constant) only interaction of electrons with the same spin leads to a renormalization of the conductance [16]. Therefore, under these conditions and in the absence of spin-flip scattering, electrons with different spin can be considered as two independent, totally spin polarized electron systems. For such a situation, one should substitute  $G_{ij}$  by  $G_{ij}/2$  in the above given expressions for the conductances leading to a semicircle relation of

the form

$$G_{xx}^2 + (G_{xy} - (2i + 1))^2 = 1 \quad (2)$$

with the vertical separatrix  $G_{xy} = 2i + 1$ .

The disordered GaAs samples were prepared by molecular-beam epitaxy. On a GaAs (100) substrate were successively grown an undoped GaAs layer (0.1  $\mu\text{m}$ ), a periodic structure of  $30 \times \text{GaAs/AlGaAs}(10/10 \text{ nm})$ , an undoped GaAs layer (0.5  $\mu\text{m}$ ), the heavily Si-doped GaAs of a nominal thickness of  $d = 27, 30, 34$  and 40 nm and a Si-donor concentration of  $1.5 \times 10^{17} \text{ cm}^{-3}$ , followed by an cap layer of 0.5  $\mu\text{m}$  undoped GaAs. The number given for a sample corresponds to the thickness of its doped layer. Hall bar geometries of width 0.2 mm and length 2.8 mm were etched out of the wafers. A phase sensitive ac-technique was used for the magnetotransport measurements down to 40 mK with the applied magnetic field up to 12 T perpendicular to the layers. For samples 27 and 30 the absolute values of the Hall resistance  $R_{xy}$  were about 10% different for two opposite directions of the magnetic field. The average has been taken as  $R_{xy}$ . The electron densities per square as derived from the slope of the Hall resistance  $R_{xy}$  in weak magnetic fields (0.5 – 3 T) at  $T = 4.2$  K are  $N_s = 3.7, 4, 5.5$  and  $6.2 \times 10^{11} \text{ cm}^{-2}$  for samples 27, 30, 34 and 40, respectively. The "bare" high temperature mobilities  $\mu_0$  are about 1300, 1400, 1900 and 2300  $\text{cm}^2/\text{Vs}$ . Because of the rather large quantum corrections to the conductivity, even in zero magnetic field at 4.2 K, we used the approximate relation  $\mu_0 = R_{xy}/BR_{xx}$  in the intersection point of the  $R_{xx}(B)$  curves for different temperatures. Previous experimental studies of the flow diagram have been performed on much purer samples with at least an order of magnitude higher mobility.

Samples 34 and 40 reveal a wide QHE plateau from  $\approx 6$  up to  $\approx 11$  T with the value  $R_{xy} = h/2e^2$  (i.e.  $i = 2$  for a spin degenerate lowest Landau-level occupation) accompanied by an exponentially small value of  $R_{xx}$  at low temperatures  $T \lesssim 0.3$  K. The magnetoresistance data of sample 40 are presented in Ref. [14].

In Fig.1 the magnetotransport data of the diagonal ( $R_{xx}$ , per square) and Hall ( $R_{xy}$ ) resistance (both given in units of  $h/e^2$ ), and of the diagonal ( $G_{xx}$ ) and Hall ( $G_{xy}$ ) conductance have been plotted for sample 30. At  $T = 4.2$  K,  $R_{xx}$  depends on magnetic field rather weakly and has only a weak minimum at  $B = 6$  T, and  $R_{xy}$  increases linearly up to 5 T with a slightly smaller slope at higher fields. Such a behaviour is typical for bulk samples in the extreme quantum limit. At the lowest temperatures, the layer is insulating ( $R \geq 100$ ) in zero magnetic field. At low magnetic fields up to 0.5 T, the diagonal resistance  $R_{xx}$  drops abruptly and continues to decrease more slowly between 0.5 and 4 T. For fields between 5 and 7 T, a minimum is observed with a QHE plateau in the Hall resistance with  $R_{xy} = 1/2$ . The same QHE

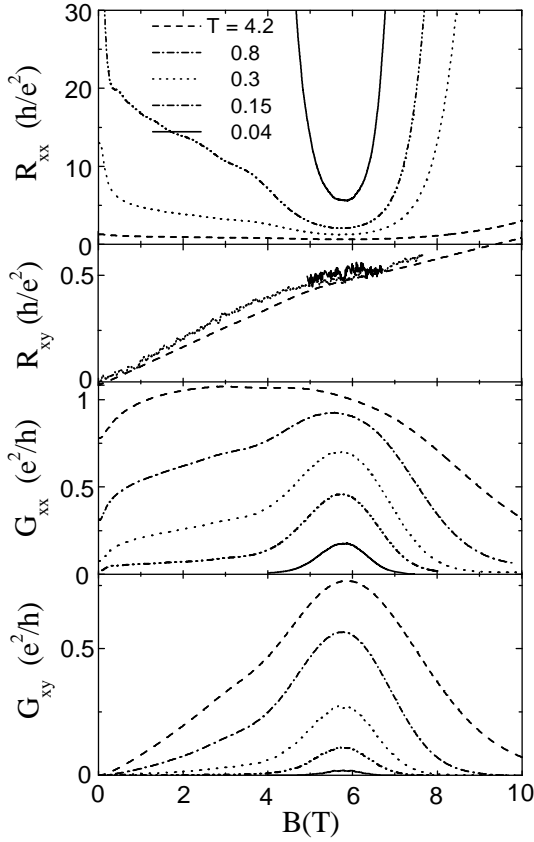


FIG. 2. Magnetic field dependence of the diagonal ( $R_{xx}$ , per square) and Hall ( $R_{xy}$ ) resistance, diagonal ( $G_{xx}$ ) and Hall ( $G_{xy}$ ) conductance for sample 27 in a magnetic field perpendicular to the heavily doped GaAs layer at different temperatures.

structure around 6 T can be observed in the plotted conductance data. In the minimum of  $G_{xx}$  near  $B = 6$  T the Hall conductance  $G_{xy}$  increases from a value higher than 1 (at 4.2 K) towards 2 at the lowest temperatures. The curves  $G_{xy}(B)$  for different temperature cross at one point with  $G_{xy} = 1$  at  $B_c = 4.9$  T. The diagonal conductivity tends towards 1 for decreasing temperature at this critical field. In this critical point the derivative  $dG_{xy}/dB$  shows a power law dependence  $\sim T^{-\mu}$  with  $\mu = 0.48 \pm 0.05$ . For curves at  $T > 0.2$  K there is a second crossing point at  $B = 7$  T with  $G_{xy} \approx 1$ . The second peak in  $G_{xx}(B)$  has an amplitude smaller than  $e^2/h$  and is broader than the first one. We believe that this second peak structure is a manifestation of spin-splitting.

In Fig.2 the magnetotransport data have been plotted for sample 27. At  $T = 4.2$  K these data are similar to the data for sample 30. However, sample 27 shows insulating behavior ( $R_{xx}$  increases with decreasing temperature) at all magnetic fields with a rather deep and narrow minimum in the field dependence  $R_{xx}(B)$  at low temperatures. Note, that at the lowest temperature we can measure  $R_{xy}$  only near the minimum of  $R_{xx}$  since outside this region  $R_{xy} \ll R_{xx}$ . Within our accuracy the

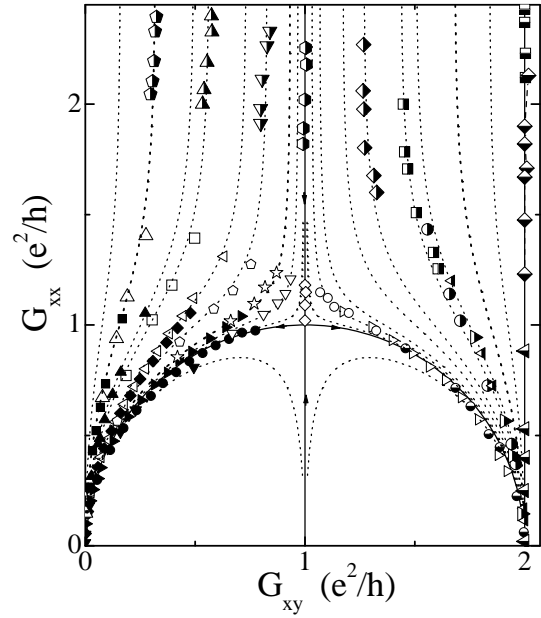


FIG. 3. Flow-diagram of the  $(G_{xx}(T), G_{xy}(T))$  data points for the investigated heavily doped GaAs layers with different thickness (filled symbols are for sample 27, open - sample 30, half right filled - sample 34 and half bottom filled - sample 40) at different magnetic field values (different type of symbols). Dotted lines show the theoretical flow lines. Solid lines display the separatrix.

sample reveals a Hall-insulator state ( $R_{xy} = 0.5$ , [6]) in this region.  $G_{xx}$  and  $G_{xy}$  have peaks at  $B \approx 6$  T.

The QHE in sample 30 is much less pronounced than in samples 34 and 40 due to the fact that the maximum of the high temperature Hall conductance  $G_{xy}^0(B)$  has a value of  $\approx 1.2$  close to 1 (see Fig.1). For  $G_{xy}^0 \rightarrow 1$  the localization length diverges, and the system is in the dissipative, non-quantized state. For samples 34 and 40 with a maximum of  $G_{xy}^0(B)$  close to 2, quantization at  $G_{xy} = 2$  develops already at higher temperatures. Although insulating for all fields, sample 27 shows a minimum in  $R_{xx}$  and a maximum in  $G_{xx}$  due to the proximity of  $G_{xy}^0(B)$  to 1 on the insulator side, giving a large localization length at its maximum.

In Fig.3 the temperature evolution of the points  $(G_{xx}(T), G_{xy}(T))$  has been plotted for the different samples at different magnetic fields taken from 4.2 down to temperatures between 0.04 and 0.1 K except for the flow lines of sample 34 in weak magnetic fields (1.4 – 2.4 T) which start only at 1.1 K. The data points at the lowest temperatures approach and, subsequently, follow the semicircle dependence given in Eq.(2). Their final low-temperature limiting value depends on the initial high temperature Hall conductance  $G_{xy}^0$  with respect to  $G_{xy} = 1$ . Data points starting on the semicircle follow this semicircle. The points starting for high temperatures at  $G_{xy} = 1$  terminate at the lowest temperatures very close to  $(G_{xx}^c, G_{xy}^c) = (1, 1)$ . The presented data on disordered

GaAs layers follow the trends expected from universal scaling arguments.

In the following we will give a quantitative estimate for the temperature dependent evolution of the flow lines at constant magnetic field. The dotted flow lines in Fig.3 are plotted as a result of a numerical solution of the equation  $\arg(f) = \alpha$  for various  $\alpha$ , where

$$f = -\vartheta_3\vartheta_4/\vartheta_2, \quad (3)$$

with the Jacobi  $\vartheta$  functions

$$\begin{aligned} \vartheta_2(q) &= 2 \sum_{n=0}^{\infty} q^{(n+1/2)^2}, & \vartheta_3(q) &= \sum_{n=-\infty}^{\infty} q^{n^2}, \\ \vartheta_4(q) &= \sum_{n=-\infty}^{\infty} (-1)^n q^{n^2}, \end{aligned} \quad (4)$$

for  $q = \exp[i\pi(G_{xy} + iG_{xx})/2]$  [7]. The value  $\alpha$  corresponds to the Hall conductance  $G_{xy}^{\infty}$  for large  $G_{xx}$  where the flow lines are vertical, with  $\alpha = \pi(1 - G_{xy}^{\infty})$  (for the flow lines above the semicircle Eq.(2)). The theoretical flow-lines are in very good agreement with the experimental data and are universally determined by the limiting  $G_{xy}^{\infty}$  values.

The rate of flow is determined by the temperature dependence of  $G_{xx}(T)$  via the parameter  $s - s_0 = \ln(f/f_0)$  where  $f_0 = f(s_0)$ . For flow along the semicircle from the critical point at (1,1), where  $f_0 = 1/4$ , we have  $s = \ln(4f)$ . In this case [7]

$$\begin{aligned} G_{xx} &= 2 \frac{K'(w)K(w)}{K(w)^2 + K'(w)^2} & G_{xy} &= 2 \frac{K'(w)^2}{K(w)^2 + K'(w)^2} \\ w &= \sqrt{\frac{1 \pm \sqrt{1 - \exp(-s)}}{2}} \end{aligned} \quad (5)$$

where  $K(w)$  is the complete elliptic function of the second kind, with  $K'(w) \equiv K(\sqrt{1-w^2})$ . The temperature dependence of  $G_{xx}$  and  $G_{xy}$  along the semicircle for samples 27, 30 and 40 can be fitted by Eq.(5) and  $s = c/T^p$  (with  $T$  in K) with  $p = 1.16, 0.94, 1.1 \pm 0.1$  and  $c = 0.83, 0.58, 3.5$ , correspondingly. For sample 30 the value of  $p$  is two times larger than the value of  $\mu = 0.48 \pm 0.05$  extracted from the temperature dependence of  $dG_{xy}/dT$ , in accordance with the proposed dependence  $s \propto (\Delta B/T^\mu)^2$  [7] ( $\mu$  is the critical exponent and  $\Delta B = B - B_c$ ). As shown in Fig. 1 the data for  $G_{xx}(B)$  and  $G_{xy}(B)$  of sample 30 at the lowest temperature are well described by Eq.(5) and  $s = 22 (\Delta B)^2$  (with  $\Delta B$  in T) around the critical point  $B_c = 4.9$  T.

For large values of  $G_{xx}$  its temperature dependence is mostly due to electron-electron interaction and the parameter  $s$  can be written as  $s = (\lambda/\pi) \ln L_T$ , where  $L_T$  is the coherence length for interaction and the constant of interaction  $\lambda$  is a material parameter which depends on magnetic field ( $\lambda < 1$ ). Note that compared to the

two-parameter scaling theory  $L_\phi$  is replaced by  $L_T$ . The interaction effects accelerate the motion along the lines.

In summary, the flow-diagram of  $(G_{xx}(T), G_{xy}(T))$  data for strongly disordered GaAs layers is well described by the universal expressions following from duality and particle-hole symmetries. Electron-electron interaction leads to an accelerated flow rate but does not change the shape of the flow lines.

This work is supported by RFBR and INTAS. We would like to thank B. Lemke for her help in the preparation of the samples.

- 
- [1] D. E. Khmel'nitskiĭ, Pis'ma Zh. Eksp. Teor. Fiz. **38**, 454 (1983) [JETP Lett. **38**, 552 (1983)]; Phys. Lett. A **106**, 182 (1984).
  - [2] H. Levine, S. B. Libby, and A. M. M. Pruisken, Phys. Rev. Lett. **51**, 1915 (1983); A. M. M. Pruisken, Nucl. Phys. **235**[FS11] 277 (1984); Phys. Rev. B **32**, 2636 (1985).
  - [3] Y. Huo, R. E. Hetzel, and R. N. Bhatt, Phys. Rev. Lett. **70**, 481 (1993).
  - [4] Igor Ruzin and Shechao Feng, Rev. Lett. **74**, 154 (1995).
  - [5] C. P. Burgess, R. Dib, and B. P. Dolan, Phys. Rev. B **62**, 15359 (2000).
  - [6] S. Kivelson, D. Lee, and S. Zang, Phys. Rev. B **46**, 2223 (1992).
  - [7] B. P. Dolan, Nucl. Phys. B **460**[FS], 297 (1999); cond-mat/9809294.
  - [8] C. P. Burgess and B. P. Dolan, Phys. Rev. B **63**, 155309 (2001).
  - [9] H. P. Wei et al., Phys. Rev. B **33**, 1488 (1988); Surf. Sci. **229**, 34 (1990); Phys. Rev. B **45**, 3926 (1992); M. Yamane et al., J. Phys. Soc. Japan **58**, 1899 (1989); S. V. Kravchenko et al., Pis'ma Zh. Eksp. Teor. Fiz. **50**, 65 (1989); S. Koch et al., Phys. Rev. B **43**, 6828 (1991); V. T. Dolgoplov et al., Zh. Eksp. Teor. Fiz. **99**, 201 (1991).
  - [10] M. Hilke et al., Nature **395**, 675 (1998).
  - [11] R. J. F. Hughes et al., J. Phys.: Condens Matter. **6**, 4763 (1994).
  - [12] R.B. Dunford, N. Griffin, and M. Pepper et al., Physica E **6**, 297 (2000).
  - [13] D. E. Khmel'nitskiĭ, Helv. Phys. Acta **65**, 164 (1992).
  - [14] S. S. Murzin, M. Weiss, A. G. M. Jansen and K. Eberl, Phys. Rev. B **64**, 233309 (2001).
  - [15] S. S. Murzin, Pis'ma Zh. Eksp. Teor. Fiz. **67**, 201 (1998) [JETP Lett. **67**, 216 (1998)].
  - [16] A. M. Finkelstein, Zh. Eksp. Teor. Fiz. **86**, 367 (1984) [Sov. Phys. JETP **59**, 212 (1984)].